Nanoscale Advances

ROYAL SOCIETY OF CHEMISTRY

COMMUNICATION

View Article Online
View Journal | View Issue

Cite this: *Nanoscale Adv.*, 2022, **4**, 2992

Received 19th May 2022
Accepted 15th June 2022

DOI: 10.1039/d2na00318j

rsc.li/nanoscale-advances

Porphyrin covalent organic nanodisks synthesized using acid-assisted exfoliation for improved bactericidal efficacy†

Xinxi Li,[a] Hajime Shigemitsu,[b] Tomoyo Goto,[ac] Toshiyuki Kida,[b] Tohru Sekino,[a] Mamoru Fujitsuka *[ad] and Yasuko Osakada *[acd]

Porphyrin covalent organic nanodisks (CONs) were synthesized by exfoliating covalent organic frameworks (COFs) in acidic aqueous solutions at pH 4. The synthesized CONs showed remarkable bactericidal activity against *Escherichia coli* owing to enhanced generation of singlet oxygen upon visible light irradiation.

Developing disinfectants is an important endeavour.[1–3] Antimicrobial materials have been developed to act against a variety of targets.[4–8] In particular, photoinactivation using photofunctional materials, such as photosensitizers, is one of the most promising methods for inactivating biological targets.[9] Among them, photofunctional organic materials, such as small molecules and polymers, are often employed as photosensitizers.[10–12] Among polymeric materials, covalent organic frameworks (COFs) are promising photocatalysts for inactivating biological targets, and thus further material development is warranted for their practical application.[13–15]

We have been studying COFs-derived organic nanomaterials such as nanodisks, and the effect of exfoliation on their photocatalytic activities in various processes, such as hydrogen production under anaerobic conditions.[16,17] As a result, we found that exfoliation occurs and photocatalytic activity is enhanced by simply stirring the material in water up to its boiling point for 20 h.[16] Recently, several groups have reported that exfoliation of imine-bound COFs is enhanced under acidic conditions such as pH 1 in organic solvents.[18,19] However, exfoliation at moderate pH in the aqueous phase has not been investigated. Additionally, inactivation of biological targets by exfoliated nanomaterials is sparsely investigated. In this study, covalent organic nanodisks (CONs) were synthesized in aqueous solutions under moderately acidic conditions to enhance their exfoliation and their photocatalytic performance during antimicrobial inactivation.

We designed CONs using porphyrin chromophores and imine linkers (Fig. 1a and b).[20] Porphyrins are one of the most promising chromophores for the photochemical inactivation of biological targets, specifically through the action of reactive oxygen species (ROS) generated upon light irradiation.[21] Therefore, in this study, the porphyrin unit was selected as the chromophore, and the imine linker was selected to form the layers in COFs, stabilized by hydrogen bonds ("locked", Fig. 1c).[20,22] To rapidly exfoliate the porphyrin COFs into nanodisks and to improve the catalytic activity of the CONs, the liquid phase was acidified (Fig. 1b). Because the pK_a of aromatic imines ranges from 5 to 7, which is sufficient to protonate the imine, protonation of the C=N bond should occur at pH 4, causing interlayer repulsion and disrupting hydrogen bonds in the flat plate to promote exfoliation ("twisted", Fig. 1c).[23]

Various techniques were used to characterize the structure of the synthesized nanodisks. The crystallinity of the CONs was

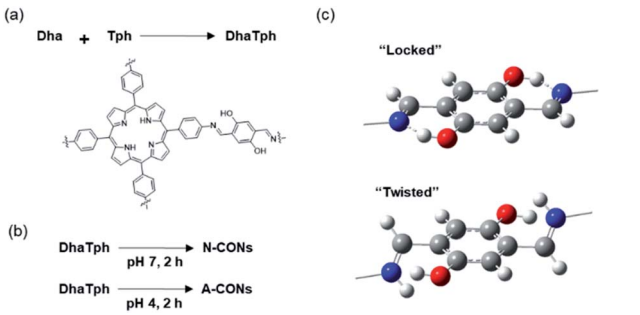

Fig. 1 (a) Synthesis scheme and chemical structure of DhaTph. (b) Synthesis scheme of N-CONs (pH 7) and A-CONs (pH 4). (c) Structures around the imine (top) and protonated imine (bottom) linkers.

[a]*SANKEN (The Institute of Scientific and Industrial Research), Osaka University, Mihogaoka 8-1, Ibaraki, Osaka 567-0047, Japan. E-mail: yosakada@sanken.osaka-u.ac.jp; fuji@sanken.osaka-u.ac.jp*

[b]*Department of Applied Chemistry, Graduate School of Engineering, Osaka University, 2-1 Yamadaoka, Suita, 565-0871, Japan*

[c]*Institute for Advanced Co-Creation Studies, Osaka University, 1-1 Yamadagaoka, Suita, Osaka, 565-0871, Japan*

[d]*Innovative Catalysis Science Division, Institute for Open and Transdisciplinary Research Initiatives (ICS-OTRI) Suita, Osaka, 565-0871, Japan*

† Electronic supplementary information (ESI) available. See https://doi.org/10.1039/d2na00318j

determined using powder X-ray diffraction (PXRD) patterns (Fig. 2a).After 2 h reaction in 0.2 M HAc/NaAc buffer at pH 4 (A-CONs), the intensity of diffraction peak at $2\theta = 3.5°$ decreased by 23% (A-CONs). In contrast, this peak decreased by 10% after 2 h in an unbuffered aqueous solution at neutral pH (N-CONs).

The surface area and porosity of the CONs were investigated using N_2 adsorption and desorption experiments. Based on adsorption/desorption isotherms, Brunauer–Emmett–Teller (BET) surface areas were determined from adsorption/desorption for isotherms (Fig. S1†). The BET surface areas were 374 $m^2\ g^{-1}$ DhaTph, 392 $m^2\ g^{-1}$ for N-CONs and 361 $m^2\ g^{-1}$ for A-CONs. The isotherms exhibited a type II behaviour and H4 type hysteresis loop, indicating that the pore structures were well preserved compared with that of DhaTph like slit type pores. The size and thickness of individual CONs were evaluated using atomic force microscopy (AFM, Fig. 2b, S2 and Table S1†). A-CONs were 58.9 ± 20.1 nm in diameter and 1.3 ± 0.8 nm in thickness. The diameter and thickness of A-CONs were respectively 20% and five times smaller than those of N-CONs (5.5 ± 7.3 nm in thickness), indicating that the acid promoted exfoliation.

The transmission electron microscopy (TEM) images (Fig. S3a†) showed that disk-shaped polymers formed. Fourier-transform infrared (FT-IR) spectra of the CONs were measured to analyse the C=N bond (Fig. 2c). The peak at 1613 cm^{-1} showed no significant difference between A-CONs and N-CONs. These results confirmed that the diameter and thickness did not decrease because of hydrolysis and bond dissociation. CHN elemental analysis was also performed and showed no significant difference among DhaTph, N-CONs, and A-CONs (Table S2†). Time-dependent analysis of PXRD patterns showed no significant crystallinity loss when the reaction time was increased to 4 h (Fig S3b†). Therefore, we exfoliated the samples under acidic conditions for 2 h. These results indicate that nanodisks can be rapidly synthesized in an acidic solution using a simple process.

As shown in Fig. 3a, the solid-state absorption spectra of CONs contain a broad absorption peak in the visible-light region. These results suggest that the newly synthesized CONs can function as a photocatalyst upon visible-light irradiation, such as for hydrogen (H_2) generation as previously described.[24] To investigate the photocatalytic properties of CONs, the H_2 generation reaction was first analyzed.[16] Synthesized CONs were hybridized with reduced graphene oxide and platinum nanoparticles (CONs/RGO/Pt), and the CONs/RGO/Pt composites were photoirradiated with a solar simulator under argon (Fig.-S4a†). We observed that the amount of H_2 produced with the composite derived from A-CONs was twice that using the composite derived from N-CONs (Fig. S4b†). Because electron transfer reactions occur at the surface, this result suggests that the surface area of the composite derived from A-CONs retains the increase surface area of A-CONs, produced *via* exfoliation under acidic conditions.

The production of ROS, namely $^1O_2$, hydroxyl radical, and superoxide ($O_2^{\bullet -}$), by light irradiation under aerobic conditions was examined to assess the bactericidal activity of the synthesized CONs.[21] Electron spin resonance (ESR) spin trapping was performed to identify the ROS.[25] As spin-trapping reagents, 4-hydroxy-2,2,6,6-tetramethylpiperidine (4-OH-TEMP) was used for $^1O_2$, and 5,5-dimethyl-1-pyrroline N-oxide (DMPO) was used for the hydroxyl radical and $O_2^{\bullet -}$ (Fig. 3b). A three-line spectral signal corresponding to 4-hydroxy-2,2,6,6-tetramethylpiperidine-*N*-oxyl was clearly observed for 4-OH-TEMP, and this

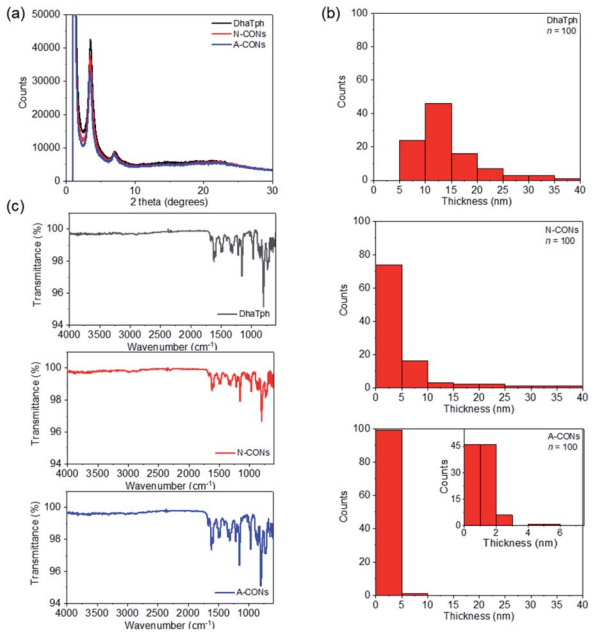

Fig. 2 (a) PXRD patterns of DhaTph, N-CONs and A-CONs. (b) Thickness distribution of DhaTph, N-CONs and A-CONs measured by AFM. (c) FT-IR spectra of DhaTph, N-CONs and A-CONs.

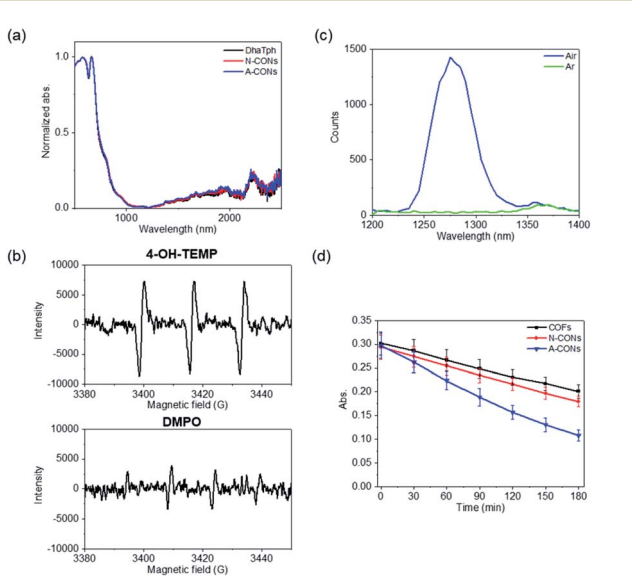

Fig. 3 (a) Normalized absorption spectra of DhaTph, N-CONs and A-CONs. (b) ESR spectra of radicals using spin-trapping reagents: 4-OH-TEMP and DMPO. A-CONs were photoirradiated in the presence of these spin-trapping reagents. (c) $^1O_2$ emission spectra from laser excitation at 532 nm. (d) DPBF chemical probe assay experiment.

signal was stronger than the DMPO signal. The formation of $^1O_2$ was also confirmed by the observation of an emission peak at 1270 nm under aerobic and argon conditions (Fig. 3c).[26] A-CONs were dispersed in toluene-h_8 and excited with a nanosecond laser (532 nm). The emission peak around 1270 nm was monitored using single-photon counting, as we previously described.[27] We observed an emission band around 1270 nm corresponding to $^1O_2$ under aerobic conditions, while no peak was observed under argon conditions (Fig. 3c). The lifetime of $^1O_2$ in toluene-h_8 under aerobic conditions was 29–31 μs, which is comparable to recent results of Ogilby *et al.* (Fig. S5†).[28]

Chemical probes were also used to evaluate the yields of $^1O_2$ and $O_2^{\bullet-}$ produced upon visible-light irradiation. 1,3-Diphenylisobenzofuran (DPBF) (Fig. 3d and S6†) and cytochrome c (Cyt c) (Fig. S6†) were used to probe $^1O_2$ and $O_2^{\bullet-}$, respectively.[15,24] For DPBF, the absorption peak at 410 nm decreased in intensity in the presence of CONs in air ($[O_2] = 2.1$ mM in methanol)[29] with increasing visible light exposure time. The apparent rate constant (k_{obs}) of the reaction with A-CONs was approximately twice as large as that with N-CONs (Fig. 3d). The k_{obs} of DPBF oxidation and apparent quantum yields are shown in Table S3.† The apparent quantum yields of $O_2^{\bullet-}$ from Cyt c assay under 1 atm of O_2 ($[O_2] = 1.27$ mM in H_2O)[29] was also determined. In the presence of $O_2^{\bullet-}$, the absorption peak at 550 nm increased when the Q-band shifted owing to the reduction of ferri-Cyt c to ferro-Cyt c (Fig. S7a†). Thus, the quantification of ROS, namely $^1O_2$ and $O_2^{\bullet-}$, indicated that $^1O_2$ was the main source of ROS under aerobic conditions.

To demonstrate the antimicrobial activity of the synthesized CONs against Gram-negative bacterium *Escherichia coli* (*E. coli*),[13] inactivation by light irradiation was evaluated. After 45 min of LED-light irradiation, a 10-fold reduction in the survival rate of *E. coli* treated with A-CONs was observed (Fig. 4 and S8†). In contrast, there was no significant decrease in the survival rate for *E. coli* treated with DhaTph and N-CONs as well as untreated *E. coli*. The morphology of *E. coli* was examined using scanning electron microscopy (SEM) (Fig. 4c and S8b†). Light-irradiated *E. coli* was fixed with aldehyde and gradually dehydrated with different concentrations of ethanol. The samples were then placed on a silicon plate and observed using SEM. The results showed that *E. coli* treated with A-CONs was damaged and morphologically altered. These results indicate that the above viability test has a threshold that impairs critical viability.

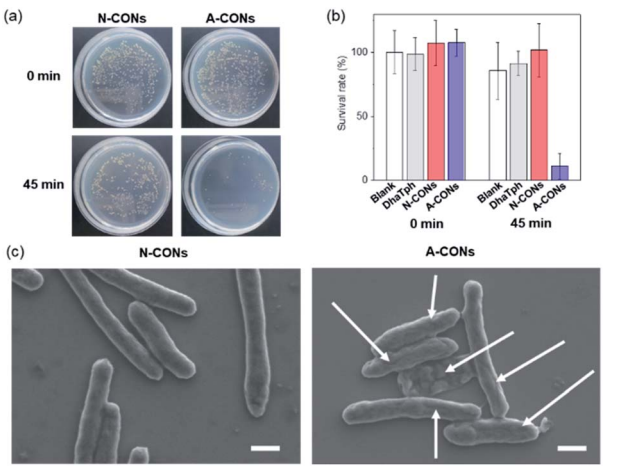

Fig. 4 (a) Representative plate photographs of *E. coli* before and after 45 min light irradiation with LED light in the presence of N-CONs and A-CONs. (b) Corresponding quantitative bacteria viability tests in the absence and presence of CONs. (c) Representative SEM images of bacteria after light irradiation in the presence of N-CONs and A-CONs. Scale bar is 1 μM. White arrows indicate the damaged area of individual *E. coli*.

Porphyrins are among the most important molecules in photodynamic therapy. When porphyrins are irradiated with visible light, triplet excited states are generated and ROS are produced by electron transfer or energy transfer. Considered the main agent of biological damage, $^1O_2$ is produced by the energy transfer to molecular O_2 with an energy level of 94 kJ mol^{-1} (type II).[30] The triplet state of free base porphyrin is 138 kJ mol^{-1}, which is sufficient to excite O_2 molecules.[31] Electron transfer and hydroxyl radical formation (type I) also competes with type II oxidation, but the present results suggest that type II is the dominant oxidation reaction under aerobic conditions using A-CONs as the photocatalyst. Regarding the bactericidal action of A-CONs, in the case of *E. coli*, $^1O_2$ caused fatal damage in the form of bacterial membrane rupture (Fig. S9 and Table S4†). The detailed mechanism underlying the primary cause of cell death will be elucidated in future studies.[32]

In summary, porphyrin nanodisks synthesized using an acid-assisted method exhibited a ten-fold increase in antimicrobial activity upon photoirradiation than nanodisks synthesized at neutral pH and original COFs.

Conflicts of interest

There are no conflicts to declare.

Acknowledgements

This work was partly supported by ENEOS TONEN General Research (Y. O.) and "Five-Star Alliance". We thank Edanz (**https://jp.edanz.com/ac**) for editing a draft of this manuscript.

Notes and references

1 H. M. Dewey, J. M. Jones, M. R. Keating and J. Budhathoki-Uprety, *ACS Chem. Health Saf.*, 2022, **29**, 27–38.
2 C. Weiss, M. Carriere, L. Fusco, I. Capua, J. A. Regla-Nava, M. Pasquali, J. A. Scott, F. Vitale, M. A. Unal, C. Mattevi, D. Bedognetti, A. Merkoci, E. Tasciotti, A. Yilmazer, Y. Gogotsi, F. Stellacci and L. G. Delogu, *ACS Nano*, 2020, **14**, 6383–6406.
3 C. Tan, C. Gao, Q. Zhou, W. Van Driel, H. Ye and G. Zhang, *RSC Adv.*, 2020, **10**, 40480–40488.
4 G. Liu, R. Yu, J. Jiang, Z. Ding, J. Ma and R. Liang, *RSC Adv.*, 2021, **11**, 4873–4882.

5 H. Yuan, H. Zhao, K. Peng, R. Qi, H. Bai, P. Zhang, Y. Huang, F. Lv, L. Liu, J. Bao and S. Wang, *ACS Appl. Mater. Interfaces*, 2020, **12**, 21263–21269.
6 B. Balasubramaniam, Prateek, S. Ranjan, M. Saraf, P. Kar, S. P. Singh, V. K. Thakur, A. Singh and R. K. Gupta, *ACS Pharmacol. Transl. Sci.*, 2021, **4**, 8–54.
7 M. Saraf, M. Tavakkoli Yaraki, Prateek, Y. N. Tan and R. K. Gupta, *ACS Appl. Nano Mater.*, 2021, **4**, 911–948.
8 Z. Usmani, T. Lukk, D. K. Mohanachandran, V. K. Thakur, V. K. Gupta, D. Robert, J. Raj, F. Scarpa and R. K. Gupta, *Curr. Res. Green Sustain. Chem.*, 2021, **4**, 100074.
9 A. Wafi, E. Szabo-Bardos, O. Horvath, M. Posfai, E. Mako, T. Juzsakova and O. Fonagy, *Nanomaterials*, 2020, **10**, 2261.
10 D. Garcia-Fresnadillo, *ChemPhotoChem*, 2018, **2**, 512–534.
11 J. Xu, Z. Wang and Y. Zhu, *ACS Appl. Mater. Interfaces*, 2017, **9**, 27727–27735.
12 Y. Liao, J. Wang, X. Song, G. Zhang and B. Chen, *Appl. Catal., B*, 2021, **292**, 120189.
13 X.-R. Chen, W.-R. Cui, R.-P. Liang, C.-R. Zhang, R.-H. Xu, W. Jiang and J.-D. Qiu, *ACS Appl. Bio Mater.*, 2021, **4**, 6502–6511.
14 D. Yan, E. Lin, F. Jin, S. Qiao, Y. Yang, Z. Wang, F. Xiong, Y. Chen, P. Cheng and Z. Zhang, *J. Mater. Chem. A*, 2021, **9**, 27434–27441.
15 N. Sun, Y. Jin, H. Wang, B. Yu, R. Wang, H. Wu, W. Zhou and J. Jiang, *Chem. Mater.*, 2022, **34**, 1956–1964.
16 X. Li, T. Goto, K. Nomura, M. Zhu, T. Sekino and Y. Osakada, *Appl. Surf. Sci.*, 2020, **513**, 145720.
17 Z. Fan, K. Nomura, M. Zhu, X. Li, J. Xue, T. Majima and Y. Osakada, *Commun. Chem.*, 2019, **2**, 55.
18 S. A. Ahmed, Q.-B. Liao, Q. Shen, M. M. F. Ashraf Baig, J. Zhou, C.-F. Shi, P. Muhammad, S. Hanif, K. Xi, X.-H. Xia and K. Wang, *Chem. –Eur. J.*, 2020, **26**, 12996–13001.
19 D. W. Burke, C. Sun, I. Castano, N. C. Flanders, A. M. Evans, E. Vitaku, D. C. McLeod, R. H. Lambeth, L. X. Chen, N. C. Gianneschi and W. R. Dichtel, *Angew. Chem., Int. Ed.*, 2020, **59**, 5165–5171.
20 S. Kandambeth, D. B. Shinde, M. K. Panda, B. Lukose, T. Heine and R. Banerjee, *Angew. Chem., Int. Ed.*, 2013, **52**, 13052–13056.
21 Y. Qian, D. Li, Y. Han and H.-L. Jiang, *J. Am. Chem. Soc.*, 2020, **142**, 20763–20771.
22 X. Chen, M. Addicoat, E. Jin, L. Zhai, H. Xu, N. Huang, Z. Guo, L. Liu, S. Irle and D. Jiang, *J. Am. Chem. Soc.*, 2015, **137**, 3241–3247.
23 J. Yang, A. Acharjya, M.-Y. Ye, J. Rabeah, S. Li, Z. Kochovski, S. Youk, J. Roeser, J. Grueneberg, C. Penschke, M. Schwarze, T. Wang, Y. Lu, R. van de Krol, M. Oschatz, R. Schomacker, P. Saalfrank and A. Thomas, *Angew. Chem., Int. Ed.*, 2021, **60**, 19797–19803.
24 X. Li, K. Nomura, A. Guedes, T. Goto, T. Sekino, M. Fujitsuka and Y. Osakada, *ACS Omega*, 2022, **7**, 7172–7178.
25 H. Shigemitsu, Y. Tani, T. Tamemoto, T. Mori, X. Li, Y. Osakada, M. Fujitsuka and T. Kida, *Chem. Sci.*, 2020, **11**, 11843–11848.
26 A. U. Khan and M. Kasha, *Proc. Natl. Acad. Sci. U. S. A.*, 1979, **76**, 6047–6049.
27 Y. Osakada, K. Kawai, T. Tachikawa, M. Fujitsuka, K. Tainaka, S. Tero-Kubota and T. Majima, *Chem. –Eur. J.*, 2012, **18**, 1060–1063.
28 M. Bregnhoej, M. Westberg, F. Jensen and P. R. Ogilby, *Phys. Chem. Chem. Phys.*, 2016, **18**, 22946–22961.
29 *Handbook of photochemistry – Third edition*, ed. M. Montalti, A. Credi, L. Prodi and M. T. Gandolfi, 2006.
30 E. F. F. Silva, C. Serpa, J. M. Dabrowski, C. J. P. Monteiro, S. J. Formosinho, G. Stochel, K. Urbanska, S. Simoes, M. M. Pereira and L. G. Arnaut, *Chem. –Eur. J.*, 2010, **16**, 9273–9286, S9273/9271-S9273/9278.
31 R. W. Redmond and J. N. Gamlin, *Photochem. Photobiol.*, 1999, **70**, 391–475.
32 B. Bocskei-Antal, A. Zolcsak, N. Kosa, I. Voszka, G. Csik, K. Toth and L. Herenyi, *Sci. Rep.*, 2019, **9**, 1–10.